Synthesis and structural characterisation of bulky heptaaromatic (hetero)aryl o -substituted s -aryltetrazines

Clève D Mboyi, Ahmad Daher, Neelab Khirzada, Charles H. Devillers, Hélène Cattey, Paul Fleurat-Lessard, Julien Roger, Jean-Cyrille Hierso

Received 00th January 20xx,
Accepted 00th January 20xx

DOI: 10.1039/x0xx00000x

Synthesis and structural characterisation of bulky heptaaromatic (hetero)aryl *o*-substituted *s*-aryltetrazines

Clève D. Mboyi,[a] Ahmad Daher,[a] Neelab Khirzada,[a] Charles H. Devillers,[a] Hélène Cattey,[a] Paul Fleurat-Lessard,*[a] Julien Roger,*[a] and Jean-Cyrille Hierso*[a]

An expedient two-steps synthesis produces in good yield polyaromatic heptacyclic (hetero)arylated *o*-substituted *s*-aryltetrazines (*s*-Tz) directly from diphenyl *s*-tetrazine. This methodology overcomes the steric limitations of classical Pinner-like syntheses encountered for *o*-functionalized *s*-Tz. A single step palladium-catalyzed *N*-directed C–H bond tetrahalogenation is followed by a Pd-catalyzed Suzuki (hetero)arylation that is achieved simultaneously on four sites. The single crystal X-ray diffraction structure of the resulting typical polyaromatic heptacyclic aromatic compound 3,6-bis(2,6-diphenyl)-1,2,4,5-tetrazine (3) is analyzed, together with *R*-functionalized peripheral phenyl derivatives [*R* = *p*-*t*-Bu (4), and *m*-OMe (10)]. Generally, stacking interactions between aromatic rings can be considerably stronger if electron-depleted rings are combined with electron-rich ones. Thus, electron-poor heteroaromatic aryltetrazines are expected to interact with electron-rich phenyl aromatic rings from reduced π…π repulsion, rendering the formation of stacking networks more favorable. Herein, despite the presence of strongly electron-deficient heteroaromatic tetrazine cores, the disruption of planarity between the various aromatic rings involved precludes the expected stacking arrangement. Thus, packing organization is driven by weak hydrogen bonding with C–H…N short contacts (or C–H…O when possible). These new heptaaromatics, which incorporate for the first time an electron-attracting nitrogen-rich core are easily modifiable from cross-coupling reactions, and constitute a relevant structural and electronical alternative to the well-known and high value class of hexaphenylbenzenes.

Introduction

Heteroaromatic compounds and biphenyls are relevant classes of scaffold for pharmaceuticals. In addition to their widely recognized bioactivity, they bind to a wide range of proteins with high levels of specificity.[1] Compounds incorporating multiple (hetero)aromatic moieties may provide useful supramolecular organization in the crystalline state because of dispersion and other weak interactions including stacking of aromatic rings, C–H…aromatic interactions, and hydrogen or halogen bonding.[2] In relation with therapeutic and materials science, further development of straightforward and atom-economic synthesis of (hetero)polyaromatic building blocks is a desirable goal, both from fundamental and industrial perspective. Among heterocyclic aromatic compounds with high nitrogen-content, 1,2,4,5-tetrazine (*s*-tetrazine, *s*-Tz) derivatives were early on discovered with the Pinner synthesis reported at the end of the nineteenth century.[3a-c] The booming of Tz applications is based on their electrochemical and photophysical properties, and their reactivity in inverse electron demand Diels–Alder (iEDDA) cycloaddition, which is compatible with biological conditions and amenable to bioconjugation.[4] *s*-Tetrazines are also used as transistors and photovoltaic devices in relation with their charge transfer properties.[5] The general syntheses of substituted *s*-aryltetrazines employ benzonitrile derivatives reacted with hydrazine in the presence of various, often hazardous, reagents.[3] A general limitation of these synthesis is their multistep processes, which overall lead to low yields. This precludes easy access to bulky *o*-substituted *s*-Tz, like the hepta(aromatic) *s*-aryl tetrazines targeted in the present work (Scheme 1, bottom left). As an alternative synthetic pathway to functionalized *s*-aryltetrazines, our group recently described their *ortho*-aryl functionalization using palladium *N*-ligand directed C–H activation, which included straightforward C–H halogenation reactions.[6] Herein, we extended our work to provide an easy synthetic access, in high yield, to unprecedented polyaromatic compounds, which combines around a linear triaromatic *p*-diaryl-tetrazine core, four (hetero)aryl moieties symmetrically arranged in *o*-aryl position (Scheme 1). The resulting heptaaromatic structure of these molecules is analogous to the one of hexaphenylbenzenes (Scheme 2), which are pertinent structuring blocks,[7,8] and precursors of many useful functional materials.[9]

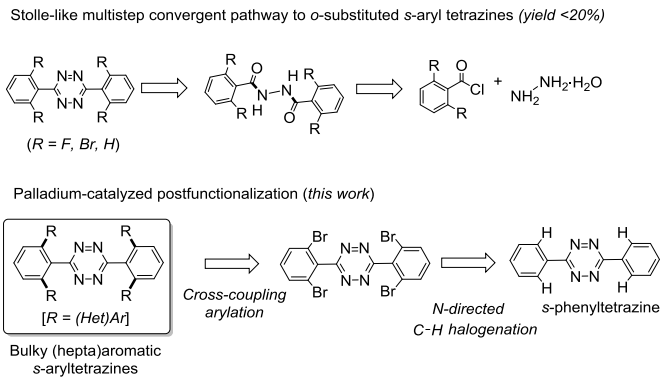

Scheme 1 Retrosynthetic strategies to hepta(aromatic) new bulky *s*-aryl tetrazines.

Palladium-catalyzed C–X bonds formation (X = OAc, I, Br, Cl, F) by *N*-directed *ortho*-C–H functionalization of *s*-aryltetrazines using a microwave-assisted synthesis allowed fast *o*-tetrabromination of *s*-phenyl tetrazine, which was used for further introducing functionalized aryl as well as heteroaryl groups. The new bulky heptaaromatic tetrazines were characterized in details by single

[a] *Institut de Chimie Moléculaire de l'Université de Bourgogne (ICMUB UMR-CNRS 6302), Université de Bourgogne Franche-Comté (UBFC) 9 avenue Alain Savary, 21078 Dijon (France)*
[b] *E-mail : paul.fleurat-lessard@u-bourgogne.fr; julien.roger@u-bourgogne.fr; hiersojc@u-bourgogne.fr*

Electronic Supplementary Information (ESI) available: Synthesis of heptaaromatic o-substituted **3**-**13**; UV-Vis measurements, Cyclic Voltammetry, Computational study (Hirshfeld surfaces and Non Covalent Interactions, NCI), Table of inter and intra-molecular interactions, and NMR spectra. See DOI: 10.1039/x0xx00000x

crystal X-ray diffraction (XRD). Their electrochemical and spectroscopic features are also reported. A special attention has been given to supramolecular organization in the crystalline state, in relation with stacking of (hetero)aromatic rings and other noncovalent weak interactions existing in such high rank polyaromatics.

Results and Discussion

Synthesis of heptaaromatic (hetero)aryl *o*-substituted *s*-aryltetrazines. Palladium-catalyzed *ortho*-C–H functionalization of 3,6-diphenyl-1,2,4,5-tetrazine **1** required overnight reaction times under classical thermal conditions.[6] We used microwave irradiation for palladium-catalyzed C–H mono- or difunctionalization –specially for fluorination– in order to decrease this reaction time at the minute scale.[6] Herein, we adapted this methodology to one-pot C–H tetrafunctionalization, with the aim of building quickly and more efficiently the valuable precursor *o*-tetrabromo-*s*-aryltetrazine **2** (Scheme 2). The reaction was optimized starting from simple 3,6-diphenyl-1,2,4,5-tetrazine **1**, in the presence of 10 mol% of $Pd(OAc)_2$ and 8 equiv. of N-bromosuccinimide (NBS). In acetic acid at 110 °C for 45 min, the 3,6-bis(2,6-dibromophenyl)-1,2,4,5-tetrazine **2** was formed and isolated pure in high 89% yield at mg scale (450 mg, 0.76 mmol). The reaction was further extended to gram scale with 79% isolated yield (2.6 g, 4.76 mmol), showing a good potential for scalability. From this convenient tetra-*o*-functionalized synthetic precursor **2** many cross-coupling reactions catalyzed by various transition metals can be envisaged. We examined Suzuki-Miyaura arylation under ligand-free palladium-catalyzed conditions (Scheme 3). A full arylation of C–Br bonds in **2** was achieved using $Pd_2(dba)_3$ in toluene at 110 °C overnight. The reaction was found to be satisfactory achieved using two equiv. of phenyl boronic acid partner and K_2CO_3 as base, with for instance **3** isolated in 95% yield. This synthetic result was remarkable since for (poly)arylation of bulky *ortho*-substituted substrates Pd-catalyzed C–C coupling often needs the assistance of bulky electron-rich phosphine or carbene ligands.[11] Herein, the aryl bromides are possibly activated by strong electron-withdrawing effect of the nitrogen-rich Tz core.

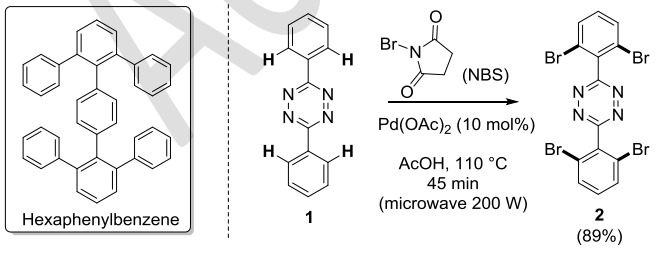

Scheme 2 Pd-catalyzed C–H *o*-bromination reaction of 3,6-diphenyl-1,2,4,5-tetrazine **1**, yielding brominated tetrazine **2** (89%).

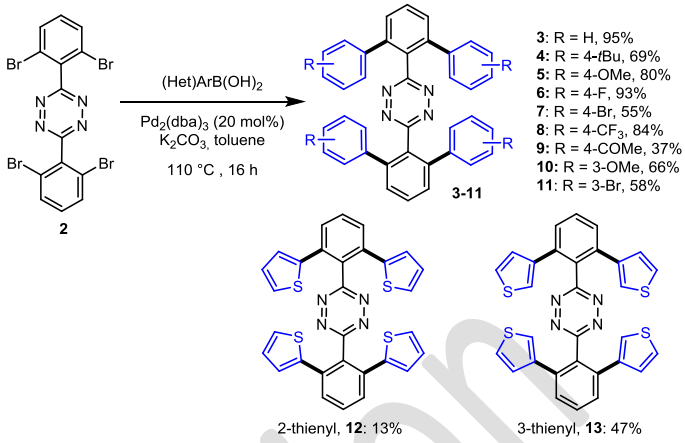

Scheme 3 Synthesis of heptaaromatic *o*-substituted *s*-aryltetrazines **3**-**13** by Suzuki-Miyaura cross-coupling using tetrabromide **2**.

With the view to develop a large set of heptaaromatic *s*-aryl tetrazine, giving thus access to a greater variety of electronic effects –including various pull-push effects from core to periphery–[12] this cross-coupling was first extended to aryl boronic acids substituted at the *para*-position. In the presence of electron-donating substituents, such as *t*-butyl and methoxy groups, the bulky heptaaromatics **4** and **5** were isolated pure in 69% and 80% yield, respectively (Scheme 3). Aryl boronic acids bearing electron-withdrawing usually "deactivating" groups were also well tolerated: the coupling of 4-fluorobenzyl boronic acid allowed the formation of compound **6** in 93% isolated yield, and the bromide analogue gave compound **7** in 55% yield. Trifluoromethylphenyl boronic acid was also a suitable coupling partner, which gave **8** in 84% yield. The coupling of 4-acetylphenyl boronic acid was achieved at 130 °C giving **9** in 37% isolated yield. Aryl boronic acids substituted in *meta*-position gave **10** in 66% yield and brominated **11** in 58% yield. These reactions also were amenable to microwave activation.[6] For instance, Suzuki-Miyaura arylation was achieved under air in toluene solvent at 90 °C, forming in 30 min the compound **4** that was isolated in 69% yield at 0.03 mmol scale.

Thiophene derivatives were also proved to be valuable heteroaryl boronic acid partners for coupling with bromoaryl *s*-Tz, giving access to unprecedented poly(hetero)aromatic *s*-phenyl tetrazines (Scheme 3).[13] Because of their strong electron-withdrawing effects, 2-thienylboronic acids were found however less reactive than the other nucleophilic aryl boronic acids we used.[14] Some additional purification troubles led to isolate the compound **12** in low yield. 3-Thienylboronic acid was found to be more convenient as a substrate, and the poly(hetero)aromatic *s*-phenyl tetrazine **13** was isolated pure in 47% yield.

Typical specimen of the set of *s*-tetrazines **1**-**13** described in the present works were crystallized as single crystals for studying and comparing by XRD their supramolecular crystalline arrangement in the solid state and assess the role of weak bonding interactions.

***o*-Substituted s-aryltetrazines structural characterization.** Noncovalent interactions (such as dispersion or hydrogen bonding) between aromatic moieties are essential in supramolecular chemistry and crystal engineering to organize molecular components in the solid state.

On one hand, *s*-Tz-based systems that include aromatic *para*-pyridinyl and *para*-pyrazinyl subunits have been examined and thoroughly described.[1] In these triaromatic systems, which are for the central core related to our present heptaaromatic *o*-(hetero)aryl *s*-Tz compounds **1**-**13**, the introduction of nitrogen heteroatoms in the scaffolds led to perturbations of aromatic interactions. The expected π–π repulsion was significantly reduced making the formation of stacked arrangements more favorable. Thus, nitrogen atoms were shown to remove electron density from the π-systems, and thus displayed a global influence analogous to electron-withdrawing groups attached on benzenes.

On the other hand, the nonplanar topologies of hexa(aryl)benzenes (Scheme 2) generally limit conjugation and disfavor extensive aromatic π…π or C–H…π interactions.[7] Compared to graphene-like fully planar analogues, such structures in which the aryl substituents are not constrained to lie in the plane of the aromatic core by supplementary bonds have weaker conjugation, and are expected to show higher HOMO–LUMO gaps, lower degrees of self-association, lesser efficient packing, and much higher solubility. These properties directly induced the recognized usefulness of non-planar phenyl-substituted benzenes in material sciences.[15]

Given that electron-poor aromatic groups may interact more strongly with electron-rich aromatic groups in stacked geometry, we were intrigued about the crystalline arrangement of heptaaromatic (hetero)aryl-*s*-aryltetrazines, as analog of hexaphenylbenzene derivatives. Are the electron-poor tetrazine core able to *intermolecular* stacking despite the bulkiness of *o*-aryl substituents? Or does these phenyl substituents control any other *intramolecular* dispersion or C–H…π interactions in some particular packing? To address these questions in detail, we studied the X-ray diffraction structures of the four structurally related *s*-aryl tetrazines (**1-Br**, **2**, **3**, **4**, and **10** in Fig. 1).

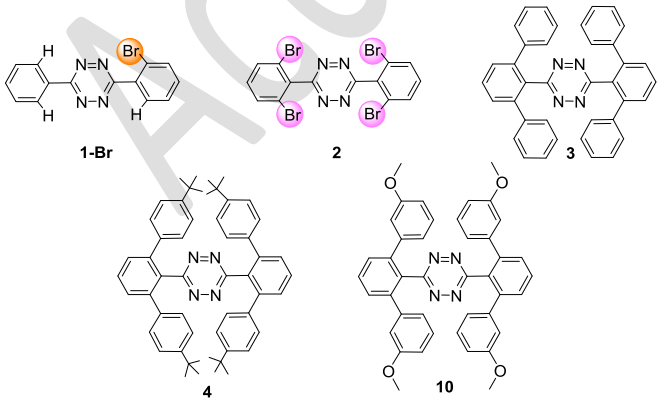

Fig. 1 Polyaromatic aryltetrazines studied by XRD.

The X-ray diffraction structure of **1-Br** (Fig. 2) illustrated a packing that reminds the arrangement found for 3,6-dipyridin-3-yl-(1,2,4,5)- tetrazine, as described by Champness *et al.*[2a] In **1-Br** the elementary motif involves two molecules which arranges head to tail, providing a favorable stacking between the phenyl (electron-rich) of one molecule and the bromophenyl (electron-poor) of the other: this arrangement is characterized with centroid–centroid distance *f* = 3.8547(13) Å for an interplanar angle between the participating phenyl rings (slippage angle) equal to 16.72°. However, a major difference for **1-Br** compared to pyridinyl-tetrazine is the absence of involvement of the tetrazine core in any strong stacking interaction, the closer tetrazine cores being separated to each other by a centroid-centroid distance *f* = 4.1285(11) Å. Some short contacts corresponding to weak intermolecular C–H···N hydrogen bonding were also observed in the packing between N3–C14, N4–C13 and N2–C5 (Fig. 2, see also ESI). Non-covalent interactions analysis also revealed C–H…Br and C–H…π interactions (see Fig S-8 and S-9 in ESI).

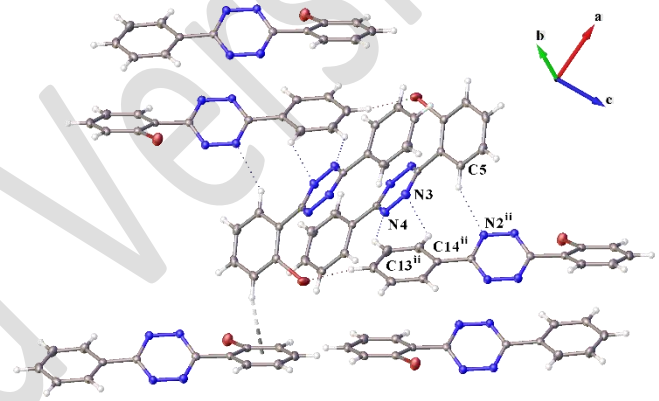

Fig. 2 Molecular structure and packing of **1-Br** (ortep with 50% probability ellipsoids). Ct1 = C1(Br)–C2–C3–C4–C5–C6, Ct2 = C7–N1–N2–N3–N4–C8 and Ct3 = C9–C10–C11–C12–C13–C14. Hydrogen atoms have been omitted for clarity. Sym. Op. (i): 1–x, 1–y, 1–z, (ii) x, 0.5-y, 0.5+z. Selected bond length (Å), angles and torsions (deg.): intermolecular Ct1–Ct3i = 3.8547(13); intermolecular Ct2–Ct2i = 4.1285(11); C1–C6–C7–N1 = 39.5(3); C1–C6–C7–N3 = –144.5(2); C5–C6–C7–N1 = –141.2(2); C5–C6–C7–N3 = 34.8(3); C10–C9–C8–N2 = 158.9(2); C10–C9–C8–N4 = –19.2(3); C14–C9–C8–N2 = –21.9(3); C14–C9–C8–N4 = 160.1(2); Intramolecular dihedral angles between Ct1 and Ct2 planes 37.06(7), and between Ct2 and Ct3 planes 21.11(7).

In the individual structure of **1-Br** molecules, the rotation of central *s*-Tz core to the *o*-bromophenyl groups attached shows a moderate distortion from planarity with intramolecular dihedral angles between the tetrazine core and bromophenyl and phenyl rings equals to 37.06(7)° and 21.11(7)°, respectively; the presence of the Br atom induces a stronger aromatic/aromatic rotational angle.

The XRD structure of the tetrabrominated synthetic precursor **2** (Fig. 3) illustrates another situation, which echoes this time the results of the Champness group for dipyrazinyl-*s*-tetrazines.[2a] In the XRD structure of **2** the elementary motif of packing involves two molecules **A** and **A**^{i} [with (i) symmetry operator: –x, 1–y, 1–z]. These molecules present *intermolecular* C–H···N short contacts between a nitrogen N2 of the Tz core of molecule **A** and a *para*-C12–H12 of

dibromophenyl of molecule **A**^{i} [dC12–H12···N2 = 3.247(3) Å, with the angle C12– H12···N2 = 109.23(16)°]. The elementary motifs are themselves linked together with an alternation of a molecule **A** and a molecule **A**^{i} by additional *intermolecular* C–H···N short contacts between N3 and C13 [dC13–H13···N3= 3.091(3) Å, with the angle C13–H13···N3 = 105.36(16)°]. Analysis of the short contact on the Hirshfeld surface also revealed an *intermolecular* halogen Br···Br bond and weak C–H···Br bonds (see also Fig S-10 and S-11 in ESI). The elementary motifs formed thus columns of alternative **A** and **A**^{i} molecules. These C–H···N, C–H···Br and Br···Br weak bondings, which

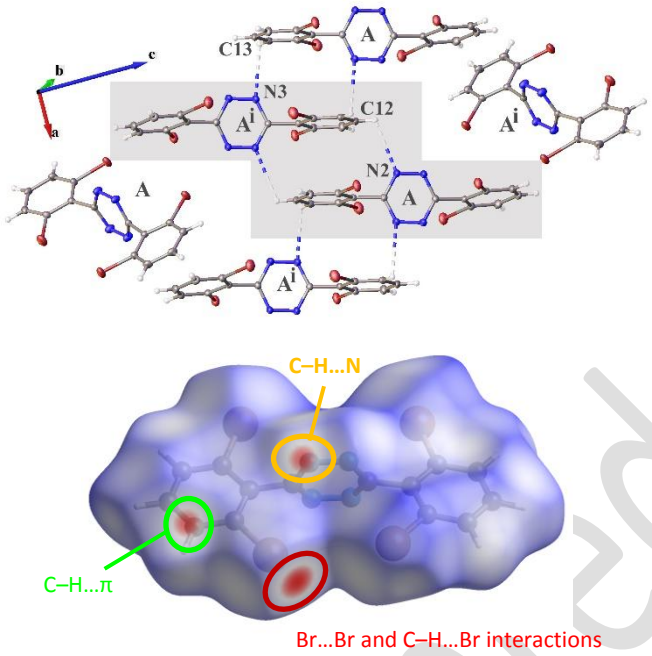

Fig. 3 Top: molecular structure and packing of **2** (ortep with 50% probability). Ct1 = C1(Br1)–C2–C3–C4–C5(Br2)–C6, Ct2 = C7–N1–N2–N3–N4–C8 and Ct3 = C9–C10(Br3)–C11–C12–C13–C14(Br4). Selected bond length (Å), angles and torsions (deg.): intermolecular Ct3-Ct3i = 3.7292(15) with (i): –x, 1–y, 1–z; C1–C6–C7–N1 = –101.3(2); C1–C6–C7–N4 = 79.3(3); C5–C6–C7–N1 = 74.3(3); C5–C6–C7–N4 = –105.1(3); C10–C9–C8–N2 = –84.0(3); C10–C9–C8–N3 = 95.1(3); C14–C9–C8–N2 = 97.5(3); C14–C9–C8–N3 = –83.4(3); intramolecular dihedral angles between Ct1 and Ct2 planes 78.15(7), and between Ct2 and Ct3 planes 83.70(7). Bottom: Hirshfeld surface of **2** mapped by the normalized distance d_{norm} (details in ESI).

seem structuring the dual molecules arrangement, are accompanied with a marked rotation of central *s*-Tz core almost perpendicularly to the *o*-dibromophenyl groups attached. Thus, the intramolecular dihedral angles between the tetrazine core and the dibromophenyl groups are respectively equals to 78.15(7)° and 83.70(7)°. In the crystal packing, the shortest centroid-centroid distance between aromatics involves two dibromophenyl groups of the elementary motif, hence **A** and **A**^{i} molecules with a Ct3–Ct3i intermolecular value *f* = 3.7292(15) Å, which clearly indicates a significant stacking interaction of aromatic rings. The corresponding interplanar distance is equal to 3.692 Å, hence the slippage angle between the normal to the planes and the centroid–centroid vector is 8.1°, corresponding to a slippage-distance of 0.53 Å. The interplanar distances between arene moieties in such kind of stacking interactions typically range within 3.3 to 3.8 Å.[16] The packing observed is also consistent with existing electrostatic interactions, as illustrated by the molecular electrostatic potential (Fig S-12 and S-13 in ESI). The analysis of the X-ray structure shows that the tetrazine core is slightly bent, resulting in a nonsymmetrical structure. Quantum calculations indicate that this bent geometry is only 0.5 kcal mol^{-1} less stable than the optimized planar one, and thus crystal packing certainly induce this low-energy distortion.

The XRD structure of the hexaphenyl-*s*-tetrazine **3** showed the presence of two different molecular conformations **A'** and **B'** in the unit cell (Fig. 4).

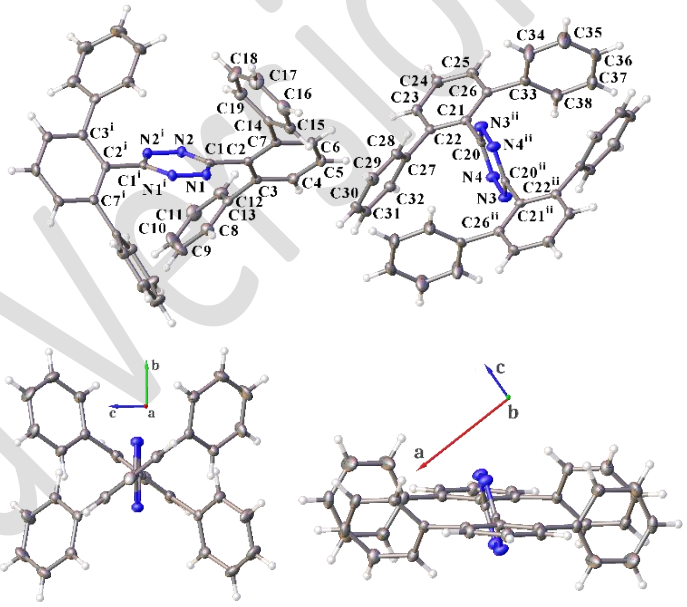

Fig. 4 Molecular structures of **3** showing 50% probability ellipsoids (**A'** left, and **B'** right). Sym. Op.: (i) 1–x, y, 1.5–z, (ii) 0.5–x, 0.5–y, 1–z. Ct1 = C2–C3–C4–C5–C6–C7, Ct2 = C1–N1–N1^{i}–N2^{i}–N2–C1, Ct3 = C21–C22–C23–C24–C25–C26 and Ct4 = C20–N4–N3–C20^{ii}–N4^{ii}–N3^{ii}). Selected angles and torsions (deg.): **A'**: C3–C2–C1–N1 = 126.2(2); C3–C2–C1–N2 = –54.0(3), C7–C2–C1–N1 = –52.5(3); C7–C2–C1–N2 = 127.3(2); **B'**: C22–C21–C20–N3^{ii}= -103.7(2); C22–C21–C20–N4 = –73.8(2); C26–C21–C20– N3^{ii} = 78.2(2); C26–C21–C20–N4 = –104.4(2); intramolecular dihedral angles between Ct1 and Ct2 planes (**A'**): 52.53(5) and between Ct3 and Ct4 planes (**B'**): 75.60(6).

The conformers **A'** and **B'** show only shallow C–H…π mutual *intermolecular* interactions (Fig. S-18) and as such their individual packing could be examined independently.

The conformer **A'** display a deviation from coplanarity of the phenyl groups attached to the *s*-Tz heteroaromatic core with a dihedral angle equals to 52.53(5)°. In conformer **A'** the central triaromatic motif diaryl *s*-tetrazine (Fig. 5) orientates the *o*-peripheral groups in directions which prevents any *intramolecular* stacking interactions (paddle-wheel like conformation, Fig. 4 bottom left), and this results in centroid-centroid distances between aromatic rings that are all above 5.0 Å. The intramolecular centroid-centroid distances between the Tz core and peripheral

phenyls are also long, being measured at values *f* = 4.3356(11) Å and 4.3373(11) Å.

In the individual packing of conformers **A'** the molecules are arranged in a parallel manner where the central tri aromatic core is roughly aligned along the ***a*** axis with the Tz core oriented quasi-perpendicular to the ***c*** axis (Fig. 6, top). In relation with the divergent orientation of peripheral phenyl groups, no *intramolecular* short C–H···N contact was detectable within conformer **A'**. However, short contacts corresponding to weak *intermolecular* C–H···N hydrogen bonding were observed in the packing (Fig. 6, bottom and Fig S-15 in ESI) between C10 and N2 type atoms, with dC10–H10···N2 = 3.357(3) and the angle C10–H10···N2 = 139.50(15)°, and between C17 and N1 type atoms with dC17–H17···N1 = 3.373(3) and the angle C17–H17···N1 = 134.66(15)°.

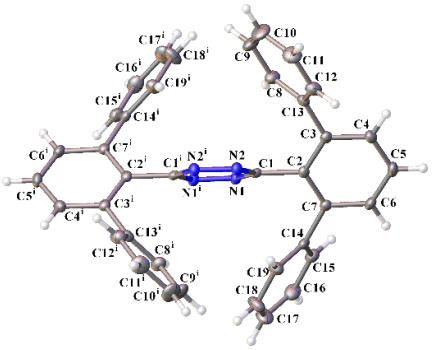

Fig. 5 Conformation of molecule **A'** for **3** showing 50% probability ellipsoids. Sym. Op.: (i) 1–x, y, 1.5–z.

In conformer **B'** a stronger deviation from coplanarity of the phenyl groups attached to the Tz heteroaromatic core is observed with a dihedral angle equals to 75.60(6)°. The arrangement displayed no *intramolecular* stacking between the arene moieties (Fig. 7) since the shortest centroid-centroid distance between proximate peripheral phenyl group was measured as *f* = 4.1720(11) Å, while distances between the Tz core and peripheral Ph groups are *f* = 4.3018(11) Å and 4.5624(12) Å. Conversely, short *intramolecular* C–H···N hydrogen bondings are detected involving two *ortho* C–H of peripheral phenyl groups: *i.e.* C28-N3^{ii} and C28^{ii}–N3 with dC–H···N= 3.287(3) Å, with the angle C–H···N = 122.79(14)° (Fig. 7).

In the individual packing of conformers **B'** (Fig. 8) the molecules are arranged in a parallel manner where the central triaromatic core is roughly aligned along the ***b*** axis, with the Tz core oriented quasi-perpendicular to the ***a*** axis direction (see also Fig. 4, bottom right).

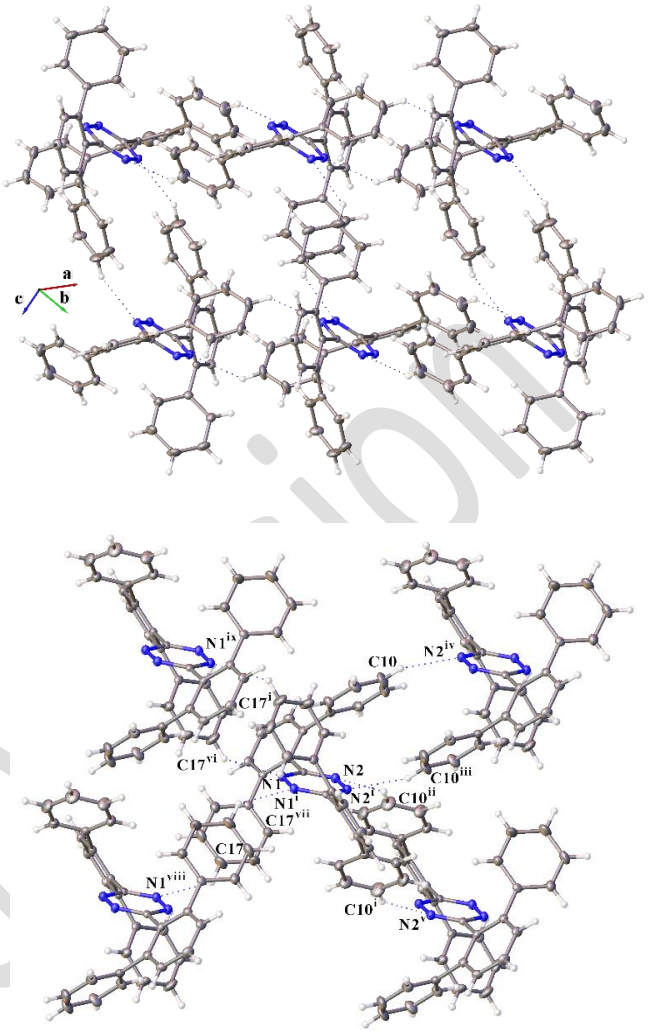

Fig. 6 View of the individual packing of conformers **A'** for **3** (top), and detail of intermolecular C–H···N hydrogen bonding network around a central molecule (bottom). Sym. Op.: (i) 1–x, y, 1.5–z, weak interactions C10-N2 : (ii) x, 2–y, -1/2+z, (iii) 1-x, 2–y, 2-z, (iv) x, 2–y, 1/2+z, (v) 1-x, 2–y, 1-z, weak interactions C17-N1 : (vi) x, –y, 1/2+z, (vii) 1-x, 1–y, 1-z, (viii) x, 1–y, -1/2+z, (ix) 1-x, 1–y, 2-z.

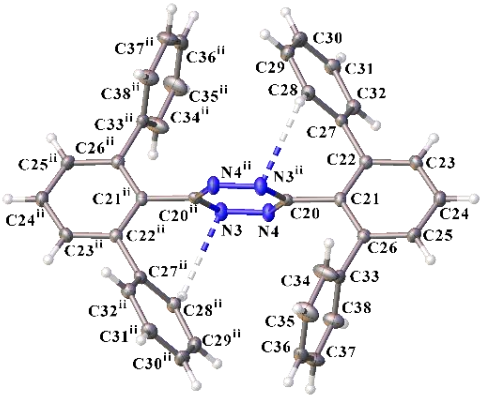

Fig. 7 Molecular structure of conformer **B'** for **3** showing 50% probability ellipsoids and short intramolecular C–H···N bonding. Sym. Op.: (ii) 1/2–x, 1/2-y, 1–z.

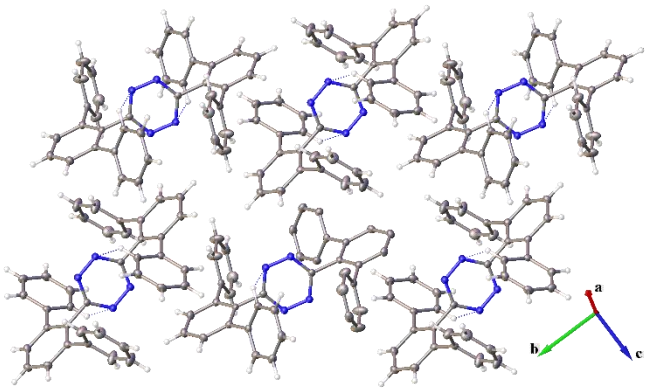

Fig. 8 View of the individual packing of conformers **B'** for **3**.

As a result, the packing of conformers **A'** and **B'** are intercalated with a highly ordered periodicity (Fig. 9). Notably, short C–H…C–H contacts exist between the central Ph groups of molecules **A'** and **B'** (d H6…H23 = 2.3 Å), as well as short contacts between their peripheral Ph groups [d C15–H···C29 = 3.697(3) and 3.758(3) Å].

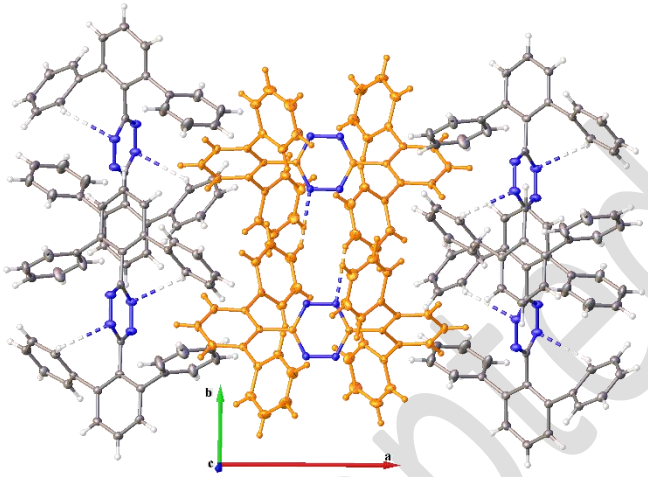

Fig. 9 Full packing of compound **3** including conformer **A'** (orange) and **B'** (grey). The weak intra- and intermolecular C–H…N interactions shown for each network of conformers participate to their well-ordered intercalation.

Thus, the heptaaromatic (hetero)aryl *s*-aryl tetrazine derivative **3** corresponds to compounds in which no long-range (or even short range) formation of structuring stacking aromatic interactions are present, despite a well-ordered crystal packing with high content in electron-poor and electron-rich aromatic rings. This absence of stacking supramolecular structuring network contrasts with the majority of simpler tetrazine analogues which have been detailed up to now, and also with the molecules reported herein **1-Br** and **2**. The strong electron-withdrawing nature of the *s*-Tz core is still insufficient in this case to force in the solid-state significant *intra-* or *intermolecular* stacking interaction.

To further study solid state crystalline arrangement in these new heptaaromatic compounds, we examined the XRD structures of the compounds **4** and **10** (Fig. 1) in which, respectively, *t*-Bu groups were introduced in *para*-position of the peripheral phenyl groups, and methoxy groups were introduced in *meta*-position of these Ph. Compound **4** is of particular interest since *t*-butyl groups, beside the additional bulkiness they provide, are known to favour in some cases structuring London dispersion forces.[17] Compounds **10** with its methoxy substitution in *meta* position is of interest to compare with both compounds **3** and **4**.

Compound **4** crystallizes as a solvate with one dichloromethane molecule (Fig. 10). No interaction between these molecules was observed. The heptaaromatic compound **4** presents a conformation reminding molecule **A'** and **B'** in compound **3**. Peripheral phenyl groups are attached to the triaromatic Ph–Tz–Ph core in a paddle-wheel like conformation precluding any *intramolecular* stacking interaction (Fig. 10). However, a lesser degree of symmetry is noted since *two* different *intramolecular* dihedral angles between axial Ph and Tz are observed: 51.64(7)° between Ct1 and Ct2 planes (torsion angle close to **A'**), and 71.38(7)° between Ct2 and Ct3 planes (torsion angle close to **B'**). In the individual packing of conformers **4** (Fig. 11),

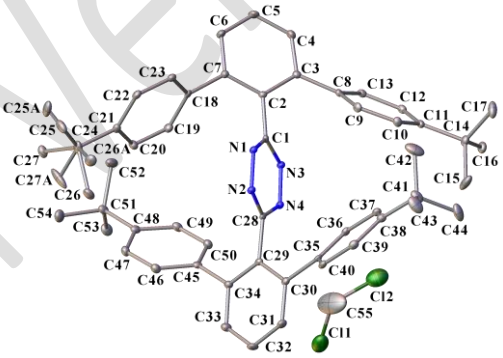

Fig. 10 Molecular structure of **4** (ortep with 50% probability, hydrogen atoms have been omitted for clarity). Ct1 = C2–C3–C4–C5–C6–C7, Ct2 = C7–N1–N2–N3–N4–C28 and Ct3 = C29–C30–C31–C32–C33–C34. Selected angles and torsions (deg.): C3–C2–C1–N1 = 130.9(2); C3–C2–C1–N3 = –48.7(3); C7–C2–C1–N1 = –53.2(3); C7–C2–C1–N3 = 127.2(2); C30–C29–C28–N2 = –70.2(3); C30–C29–C28–N4 = 106.5(2); C34–C29–C28–N2 = 109.6(2); C34–C29–C28–N4 = –73.7(3); Intramolecular dihedral angles between Ct1 and Ct2 planes 51.64(7) and between Ct2 and Ct3 planes 71.38(7).

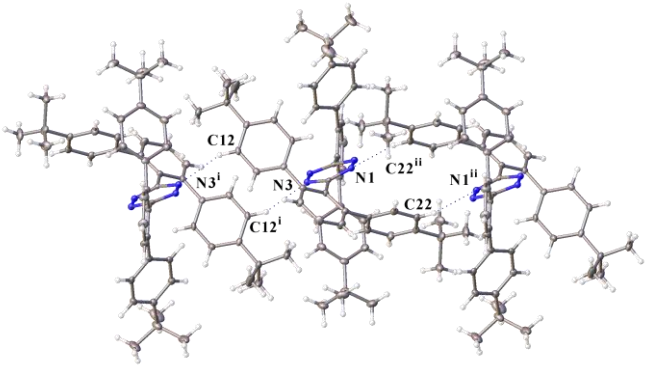

Fig. 11 Global arrangement in **4** (showing 50% probability ellipsoids, the minor part of the disordered *t*-butyl groups and the dichloromethane molecules have been omitted for clarity) with short intermolecular C–H···N

bonding. Sym. Op. in weak interactions N3–C12: (i) 1–x, 1–y, –z, and weak interactions N1–C22: (ii) 1–x, 1–y, 1–z.

the molecules can be viewed as arranged in a parallel manner along the ***a*** axis, with a distance between two *s*-Tz core *f* = 11.4653(11) Å, or along the ***b*** axis with a distance between two *s*-Tz core equal *f* = 12.8803(11) Å, evidencing a steric effect of the bulky *t*-Bu groups. Because of the orientation of the *o*-peripheral groups, the crystal packing did not display any *intramolecular* stacking interaction between the arene moieties: the centroid-centroid distance between proximate peripheral phenyl groups and Tz core were measured as *f* = 4.1555(12) Å and 4.1674(12) Å, and between the Tz core and peripheral phenyls as lying in the range *f* = 4.2985(12) to 4.5187(12) Å. Conversely, short contacts corresponding to weak *intermolecular* C–H···N hydrogen bonding were observed in the packing (Fig. 11) between C12 and N3 type atoms, with d C12–H12···N3 = 3.442(3) and the angle C12–H12···N3 = 155.83(15)°, and between C22 and N1 type atoms with d C22–H22···N1 = 3.527(3) and the angle C22–H22···N1 = 167.26(14)°.

The XRD structure of compound **10** presents a highly symmetrical paddle-wheel like conformation (Fig. 12) similar to the one found for conformer **A**' in **3** in which intramolecular dihedral angles between Ct1 and Ct2 planes equals 59.93(4). With the two methoxyphenyl groups hold in *meta*-position of the four peripheral phenyl groups linked to the central triaromatic core, no *intramolecular* stacking interaction is achieved.

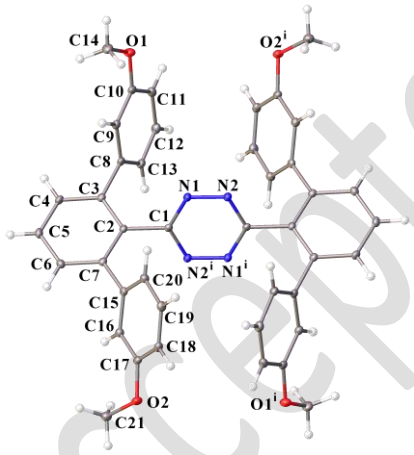

Fig. 12 Molecular structure of **10** (ortep with 50% probability). Ct1 = C2–C3–C4–C5–C6–C7, Ct2 = C1–N1–N2–C1^{i}-N1^{i}–N2^{i}. Selected angles and torsions (deg.): C3–C2–C1–N1 = 60.89(15); C3–C2–C1–N2^{i} = –118.51(12); C7–C2–C1–N1 = –120.70(12); C7–C2–C1–N2^{i} = 59.91(14); intramolecular dihedral angles between Ct1 and Ct2 planes: 59.93(4).

In the crystal packing (Fig. 13), molecules can be viewed as arranged in a parallel manner along the ***a*** axis, with a distance between two Tz core centroids equal to 11.6114(6) Å, or along the ***b*** axis with a much shorter distance equal to 7.0737(6) Å. Despite a steric congestion lesser than compound **4**, in the crystals of compound **10** *intermolecular* stacking interaction are also absent. Indeed, the *intermolecular* centroid-centroid distance between proximate phenyl groups and the Tz core was measured as *f* = 4.1870(6) Å, and between the Tz core and peripheral methoxyphenyl groups as *f* = 4.4259(6) Å and 4.4587(6) Å.

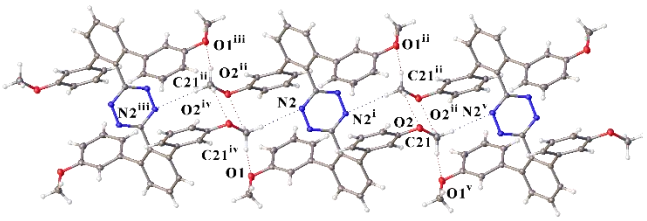

Fig. 13 Global arrangement in **10** (showing 50% probability ellipsoids) along the **b** axis with short intermolecular C–H···N and C–H···O bonding. Sym. Op.: (i) 1–x, 1–y, 1–z; weak interactions N2–C21, C21–O1, C21–O2: (ii) 2–x, 1–y, 1–z; (iii) –x, 1–y, 1–z; (iv) –1+x, y, z; (v) 1+x, y, z.

In the packing, molecules are linked together via two types of weak *intermolecular* interactions (Fig. 13): C–H···N and C–H···O hydrogen bonding around the C21 atom. Hence, the N2–C21 distance is equal to 3.7238(16) Å with an angle N2–H21–C21 = 176.41(7), the O1–C21 distance equals 3.3735(16) Å with an angle of 123.25(8)°, and the O2–C21 distance equal to 3.4858(15) Å with an angle of 143.03(7)°.

Overall, the XRD analysis of the functionalized heptaaromatics **4** and **10** confirmed that their ordered crystal packing, despite a high content in aromatic rings including electron-poor *s*-Tz, do not favour long-range structuring from stacking of aromatic rings. Instead a variety of hydrogen bondings involving nitrogen or oxygen atoms are strongly involved in the supramolecular arrangement of these polyaromatics.

Electrochemical and UV-vis feature of heptaaromatic aryltetrazines. Cyclic voltammetry analysis of **1-5**, **7**, **8**, **10** and **11** in CH_2Cl_2 0.1 M tetra-*n*-butylammonium hexafluorophosphate ($TBAPF_6$) is shown in ESI (Fig. S-4 to S-6 and Tables S-2 to S-4). Illustrative cyclic voltammetry analysis of **3**, **4** and **8** is presented in Fig. 14. Potentials are given *vs* the saturated calomel electrode (the Fc^+/Fc redox couple appears at 0.46 V *vs* SCE in these conditions).

The redox behavior of **3**, **4** and **8** is similar. A multi-electronic and irreversible oxidation process is observed at $E_{pa} \approx 2.0$ V for all compounds. This irreversible behavior occurring consecutively to the electron transfer is tentatively attributed to the oxidative C–C coupling of the phenyl rings *via* an EC mechanism. The presence of *t*-butyl groups in **4** compared to **3** does not induce significant difference in their oxidation potential. Conversely, the mono-electronic reversible tetrazine core centered reduction, which leads to the corresponding anion radical,[3i,18] takes place at a more negative potential in **4** ($E_{1/2}$ = −1.09 V, ΔE_p = 105 mV) than in **3** ($E_{1/2}$ = −0.98 V, ΔE_p = 95 mV), this is consistent with the electron-donating inductive effect of the *t*-butyl groups. As **8** bears electron-withdrawing groups, its reduction takes place at a less negative potential ($E_{1/2}$ = −0.88 V, ΔE_p = 170 mV) than in **3** and **4**.

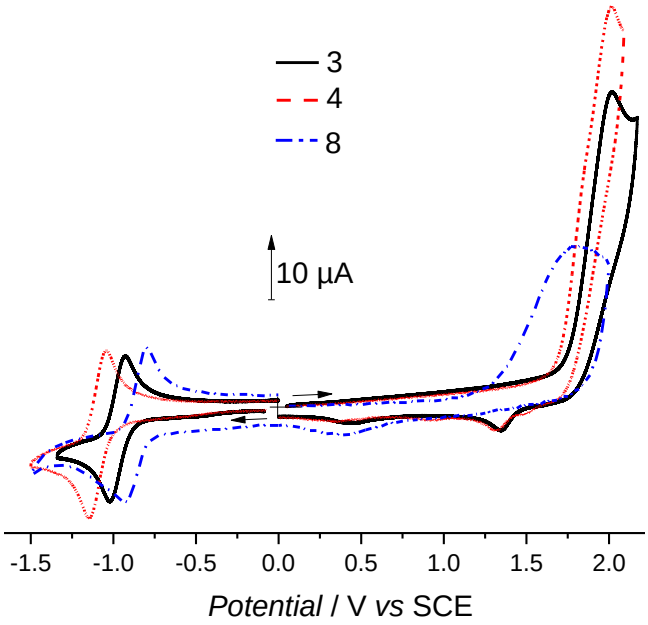

Fig. 14 Cyclic voltammetry for **3** (black line), **4** (red dashed line) and **8** (blue dotted line) in CH_2Cl_2 0.1 M $TBAPF_6$. Concentration: 10^{-3} M; WE: glassy carbon Ø = 3 mm, v = 100 mV s^{-1}.

The UV-vis absorption data of compounds **2**-**13** in dichloromethane are collected in Table 1 (see also Table *S-1*, and Fig. *S-1 to S-3* in ESI). Illustrative absorption spectra are depicted in Fig. 15. The 3,6-bis (2,6-dibromophenyl)-1,2,4,5-tetrazine **2** displays two intense absorption bands at 260 and 532 nm with the respective molar extinction coefficients Ɛ (9252 and 515 L mol^{-1} cm^{-1}). These absorptions are respectively attributed to the π–π* transitions centered on tetrazine and aryl groups and n–π* centered on the tetrazine ring.[4,5b] The heptaaromatic tetrazines **3**-**13** display similar spectral profile with two absorption maxima at *c.a.* 300 nm and 550 nm. The corresponding molar absorption coefficient varies between 11069 to 25120 L mol^{-1} cm^{-1} depending on the nature and the position of the substituents carried by the aryl moieties for the π–π* transitions. For the second band n–π* charge transfer band, localized around 550 nm, a weaker molar absorption coefficient is observed (652 to 933 L mol^{-1} cm^{-1}).

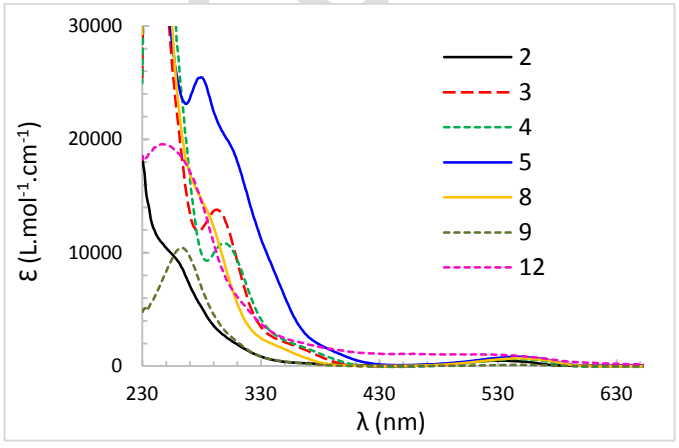

Fig. 15 Molar absorption coefficient of compounds of tetrazines **2,-5,8,9** and **12** in dichloromethane at about 8.0-9.0.10^{-5} M.

Table 1 Photophysical properties for compounds **2-13** in dichloromethane: Absorption wavelength (λ, nm) molar absorption coefficient (Ɛ, L mol^{-1} cm^{-1}).

Tz	λ_1 (nm)	ε_1 (λ_1) (L mol^{-1} cm^{-1})	λ_2 (nm)	ε_2 (λ_2) (L mol^{-1} cm^{-1})
2	260	9 253	532	515
3	296	13 910	550	700
4	302	11 069	548	696
5	282	25 120	548	771
6	284	11 458	549	732
7	294	11 285	549	796
8	284	14 270	549	652
9	265	10 456	550	594
10	281	21 369	548	652
11	295	12 577	550	752
12	243	19 330	522	933
13	291	11 845	547	807

Conclusions

We reported an expedient two-steps synthesis of heptacyclic (hetero)arylated *o*-substituted *s*-aryltetrazines (**3**-**13**) directly from one-pot four sites C–H bromination of diphenyl *s*-tetrazine, followed by one-pot four sites arylation at bromides by Suzuki-Miyaura cross-coupling. These new heptaaromatic compounds incorporate for the first time an electron-attracting tetrazine nitrogen-rich core. They are easily modifiable from cross-coupling reactions, and are relevant analogs of high-value nonplanar hexaphenylbenzenes.

The electrochemical and spectroscopic features of compounds **3**-**13** are typical of *s*-aryltetrazines. However, their supramolecular organization in the crystalline state, thoroughly investigated in relation with dispersive stacking and noncovalent weak interactions (such as C–H…N, C–H…π, hydrogen or halogen bonding) in high rank polyaromatics, showed that despite the presence of a strongly electron-deficient heteroaromatic tetrazine core and multiple phenyl groups, no significant intra- and intermolecular stacking interactions of aromatic rings exist –at least in the representative examples **3**, **4** and **10**–. A net disruption of planarity between the *o*-connected aromatic rings in individual molecules (paddle wheel-like conformation) was observed and the packing organization is driven by weak hydrogen bonding with C–H…N short contacts (or C–H…O when possible). In particular, in the global crystal packing of **3**, a very intricate intercalation between two conformationally distinct *s*-Tz molecules arranged in individual networks was analyzed. These features are relevant for further construction of electron-poor, non-planar phenyl-substituted benzenes, obviously complementary to graphene-like fully planar building blocks in materials science.

Acknowledgements

This work was supported by the CNRS, Université de Bourgogne, Conseil Régional de Bourgogne (I-SITE program COMICS for J.-C. H.) and the fonds Européen de Développement Regional (FEDER) programs, by the COMUE UBFC (I-SITE UB180013.MUB. IS_SmartTZ for J. R.; PhD grant for A. D.) and by the ANR JCJC (ANR-18-CE07-0015 – FIT-Fun for J. R.) and (ANR-15-CE29-0018-01 – Porfusion for C. H. D.). Calculations were performed using HPC resources from DNUM CCUB (Centre de Calcul de l'Université de Bourgogne).

Notes and References

‡ CCDC 1559131 (**1-Br**), 1559130 (**2a**), 1559132 (**3a**), 1991440 (**4**),1993888 (**10**) contains the supplementary crystallographic data for this paper. These data can be obtained free of charge from The Cambridge Crystallographic Data Centre *via* www.ccdc.cam.ac.uk/data_request/cif.

1 (*a*) J. S. Carey, D. Laffan, C. Thomson, and M. T. Williams, *Org. Biomol. Chem.*, 2006, **4**, 2337; (*b*) H. Doucet and J.-C. Hierso, *Curr. Opin. Drug Discovery Dev.*, 2007, **10**, 672; (*c*) D. A. Horton, G. T. Bourne and M. L. Smythe, *Chem. Rev.* 2003, **103**, 893; (*d*) P. J. Hajduk, M. Bures, J. Praestgaard and S. W. Fesik, *J. Med. Chem.* 2000, **43**, 3443.

2 (*a*) N. S. Oxtoby, A. J. Blake, Neil R. Champness and C. Wilson, *CrystEngComm*, 2003, **5**, 82, and references cited therein. Note that discussions exist on the nature of stacking interactions between aromatic rings and the way of naming it. Grimme and others recommended to restrict the term π…π stacking to large unsaturated systems close in space. The term "stacking of aromatic rings" herein is preferred, see: (*b*) S. Grimme, *Angew. Chem. Int. Ed.* 2008, **47**, 3430; (*c*) C. R. Martinez and B. L. Iverson, *Chem. Sci.* 2012, **3**, 2191; (*d*) K. Molčanov, V. Milašinović and B. Kojić-Prodić, *Cryst. Growth Des.* 2019, **19**, 5967–5980.

3 (*a*) A. Pinner, *Chem. Ber.,* 1893, **26**, 2126; (*b*) A. Pinner, *Chem. Ber.,* 1897, **30**, 1871; (*c*) R. Stollé, *J. Prakt. Chem.,* 1906, **73**, 277; (*d*) Y. Qu, F.-X. Sauvage, G. Clavier, F. Miomandre and P. Audebert, *Angew. Chem. Int. Ed.,* 2018, **37**, 12233; (*e*)W. Mao, W. Shi, J. Li, D. Su, X. Wang, L. Zhang, L. Pan, X. Wu and H. Wu, *Angew. Chem. Int. Ed.,* 2018, **37**, 12233; (*f*) C. Li, H. Ge, B. Yin, M. She, P. Liu, X. Li and J. Li, *RSC Adv.,* 2015, **5**, 12277; (*g*) H. Liu and Y. Wei, *Tetrahedron Let.,* 2013, **54**, 4645; (*h*) J. Yang, M. R. Karver, W. Li, S. Sahu and N. K. Devaraj, *Angew. Chem. Int. Ed.,* 2012, *51*, 5222; (*i*) P. Audebert, S. Sadki, F. Miomandre, G. Clavier, M. C. Vernières, M. Saoud, P. Hapiot, *New. J. Chem.,* 2004, **28**, 387.

4 (*a*) G. Clavier and P. Audebert, *Chem. Rev.* 2010, **110**, 3299; (*b*) N. K. Devaraj and R. Weissleder, *Acc. Chem. Res.* 2011, **44**, 816; (*c*) R. P. Singh, R. D. Verma, D. T. Meshri and J. M. Shreeve, *Angew. Chem. Int. Ed.* 2006, **45**, 3584; (*d*) W. Kaim, *Coord. Chem. Rev.* (*e*) N. Saracoglu, *Tetrahedron*, 2007, **63**, 4199.

5 (*a*) M. Moral, G. García, A. Garzon, J. M. Granadino-Roldan, M. A. Fox, D. S. Yufit, A. Penas, M. Melguizo and M. Fernandez-Goez *J. Phys. Chem., C* 2014, **118**, 26427; (*b*) C. Quinton, V. Alain-Rizzo, C. Dumas-Verdes, G. Clavier, L. Vignau and P. Audebert *New J. Chem.,* 2015, **39**, 9700; (*c*) Y. Qu, Piotr Pander, O. Vybornyi, M. Vasylieva, R. Guillot, F. Miomandre, F. B. Dias, P. Skabara, P. Data, G. Clavier and Pierre Audebert *J. Org. Chem.,* 2020, **85**, 3407

6 C. Testa, E. Gigot, S. Genc, R. Decréau, J. Roger, J.-C. Hierso *Angew. Chem. Int. Ed.,* 2016, **55**, 5555; J.-C. Hierso, J. Roger, C. Testa, R. Decréau, *US Pat. Appl.*, 2015, US 62/260,741; J.-C. Hierso, J. Roger, C. Testa, R. Decréau, *PCT Int. Appl.* 2017, WO 2017093263 A1 20170608; C. D. Mboyi, C. Testa, S. Reeb, S. Genc, H. Cattey, P. Fleurat-Lessard, J. Roger and J.-C. Hierso, *ACS Catal.,* 2017, **7**, 8493; C. D. Mboyi, D. Vivier, A. Daher, P. Fleurat-Lessard, H. Cattey, C. H. Devillers, C. Bernhard, F. Denat, J. Roger, J.-C. Hierso, *Angew. Chem. Int. Ed.,* 2020, **59**, 1149.

7 (*a*) D. Gust, *J. Am. Chem. Soc.* 1977, **99**, 21; (*b*) E. Gagnon, T. Maris, P.-M. Arseneault, K. E. Maly and J. D. Wuest, *Cryst. Growth Des.,* 2010, **10**, 648.

8 S. J. Emond, P. Debroy and R. Rathore, *Org. Lett.*, 2008, **10**, 389.

9 Y. Hu, X.-Y. Wang, P.-X. Peng, X.-C. Wang, X.-Y. Cao, X. Feng, K. Müllen and A. Narita, *Angew. Chem. Int. Ed.,* 2017, **56**, 3374.

10 Q. Zhong, Y. Hu, K. Niu, H. Zhang, B. Yang, D. Ebeling, J. Tschakert, T. Cheng, A. Schirmeisen, A. Narita, K. Müllen and L. Chi, *J. Am. Chem. Soc.,* 2019, **141**, 7399.

11 See for a recent example including pertinent referencing: D., Shen, Y. Xu and S.-L. Shi, *J. Am. Chem. Soc.,* 2019, **141**, 14938.

12 Donor-acceptor organic compounds exhibiting charge-transfer transitions are valuable systems for thermally activated delayed fluorescence (TADF) materials related to organic light-emitting diode (OLED) and other electroluminescent devices, for a recent review, see: Y. Wong and E. Zysman-Colman, *Adv. Mater.,* 2017, **29**, 1605444.

13 Thienyl-*s*-tetrazine have shown interesting electronic properties for material devices, see: (*a*) Z. Li, J. Ding, N. Song, J. Lu and Y. Tao, *J. Am. Chem. Soc.,* 2010, **132**, 13160; (*b*) J. Ding, Z. Li, Z. Cui, G. P. Robertson, N. Song, X. Du and L. Scoles *J. Polym. Sci. Part. A Polym. Chem.,* 2011, **49**, 3374; (*c*) E. Kurach, D. Djurado, J. Rimarcik, A. Kornet, M. Wlostowski, V. Lukes, J. Pécaut, M. Zagorska and A. Pron *Phys. Chem. Chem. Phys.,* 2011, **13**, 2690; (*d*) Q. Ye, W. T. Neo, C. M. Cho, S. W. Yang, T. Lin, H. Zhou, H. Yan, X. Lu, C. Chi and J. Xu *Org. Lett.,* 2014, **16**, 6386.

14 M. Melucci, G. Barbarella and G. Sotgiu, *J. Org. Chem.,* 2002, **67**, 8877.

15 (*a*) U. Kumar, T. X. Neenan, *Macromolecules,* 1995, **28**, 124; (*b*) A. Pogantsch, F. P. Wenzl, E. J. W. List, G. Leising, A. C. Grimsdale, K. Müllen, *Adv. Funct. Mater.,* 2002, 1**4**, 1061; (*c*) F. Chiaravalloti, L. Gross, K.-H. Rieder, S. M. Stojkovic, A. Gourdon, C. Joachim and F. Moresco, *Nat. Mater.,* 2007, **6**, 30; (*d*) W. Xiao, X. Feng, P. Ruffieux, O. Gröning, K. Müllen and R. Fasel, *J. Am. Chem. Soc.,* 2008, **130**, 8910; (*e*) M. Hoffmann, J. Kärnbratt, M.-H. Chang, L. M. Herz, B. Albinsson and H. L. Anderson, *Angew. Chem. Int. Ed.,* 2008, **47**, 4993; (*f*) M. A. Alam, Y.-S. Kim, S. Ogawa, A. Tsuda, N. Ishii and T. Aida, *Angew. Chem. Int. Ed.,* 2008, **47**, 2070; (*g*) S. Hiraoka, K. Harano, T. Nakamura, M. Shiro and M. Shionoya, *Angew. Chem. Int. Ed.,* 2009, **48**, 7006.

16 (*a*) C. Janiak, *J. Chem. Soc., Dalton Trans.* 2000, 3885; (*b*) J. G. Planas, C. Masalles, R. Sillanpää, R. Kivekäs, F. Teixidor and C. Viñas, *CrystEngComm*, 2006, **8**, 75.

17 J. P. Wagner, P. R. Schreiner, *Angew. Chem. Int. Ed.,* 2015, **54**, 12274.

18 R. Gleiter, V. Schehlmann, J. Spanget-Larsen, H. Fischer and F. A. Neugebauer, *J. Org. Chem.*, 1988, **53**, 5756.